

Article

An Ab Initio Investigation of the Hydration of Tin(II)

Cory C. Pye *  and Champika Mahesh Gunasekara

Department of Chemistry, Saint Mary's University, Halifax, NS B3H 3C3, Canada

* Correspondence: cory.pye@smu.ca

Abstract: The structure of tin(II) is not well known in aqueous solution. The energies, structures, and vibrational frequencies of $[\text{Sn}(\text{H}_2\text{O})_n]^{2+}$ $n = 0-9$, 18 have been calculated at the Hartree-Fock and second order Møller-Plesset levels of theory using the CEP, LANL2, and SDD effective core potentials in combination with their associated basis sets, or with the 6-31G* and 6-31+G* basis sets. The tin-oxygen distances and totally symmetric stretching frequency of the aquatin(II) ions were compared with each other, and with solution measurements where available.

Keywords: ab initio; tin(II); hydration; symmetry; vibrational spectrum

1. Introduction

The structure of some metal ions in solution remain elusive [1,2]. Their toxicity to man and the environment is dependent on their oxidation state and speciation, which often depends on pH and the presence of counterions that solubilize the metal by complex formation. Computational chemistry can be useful in supporting and rationalizing proposed speciation models. However, for elements of high atomic number, a drawback is that there are typically few all-electron basis sets that can be used, and relativistic effects can play an important role. One workaround is to use effective core potentials, which replace the explicit description of core electrons by a core potential, which are then paired with basis sets describing the outermost electrons. Previously, some common effective core potentials for the aqua complexes of the heavy metals mercury(II) and thallium(III) (valence electron configuration $5d^{10}$) were benchmarked [3]. This work was extended to lead(II) with a valence electron configuration of $6s^25d^{10}$ [4]. We expand our work now to tin(II), which has a valence electron configuration of $5s^24d^{10}$. The presence of the ns^2 subshell, as with lead(II), will be shown to have a pronounced effect on the structures compared to those without it. *Hemidirected* structures (which tend to be favored at lower coordination numbers) have ligands that are not symmetrically distributed around the central ion, whereas *holodirected* structures have a symmetrical distribution.

In the gas-phase, it was reported that tin(II), lead(II), and mercury(II) easily underwent a proton transfer reaction and that the only species observed in the mass spectra were the deprotonated $\text{MOH}^+(\text{H}_2\text{O})_{n-1}$ ions, not the $\text{M}(\text{H}_2\text{O})_n^{2+}$ ions. These ions have anomalously high acidity in the gas phase as well as the solution phase. An ab initio study was carried out to rationalize this behavior, with a focus on the pathways to deprotonation [5]. In solution, it is believed that the relevant species are $\text{Sn}^{2+}(\text{aq})$ (pH < 2), $\text{SnOH}^+(\text{aq})$, $\text{Sn}_2(\text{OH})_2^{2+}(\text{aq})$, $\text{Sn}_3(\text{OH})_4^{2+}(\text{aq})$, $\text{Sn}(\text{OH})_2^0(\text{aq})$ (pH = 5–8), and $\text{Sn}(\text{OH})_3^-(\text{aq})$ (pH > 10) [2]. The polynuclear species form at higher concentrations, and the water content cannot be determined through potentiometric means.

The tin(II) ion in aqueous solution has been characterized by an X-ray study of a ~ 3 mol/L solution of the perchlorate salt [6]. The radial distribution curves showed peaks at 1.4 Å (Cl–O), 2.3 Å (O...O and Sn–O), 2.8 Å (Sn–O), 3.6 Å (Sn–Sn), and 4.2 Å (Sn...O). Some hydrolyzed solutions were also examined, and the largest variation was in the 3.6 Å and 4.2 Å peaks, which suggested a greater degree of clustering as the hydrolysis increased. Essentially the same unhydrolyzed solution was studied by EXAFS [7], in which a Sn–O



Citation: Pye, C.C.; Gunasekara, C.M. An Ab Initio Investigation of the Hydration of Tin(II). *Liquids* 2022, 2, 465–473. <https://doi.org/10.3390/liquids2040027>

Academic Editor: Enrico Bodo

Received: 24 November 2022

Accepted: 8 December 2022

Published: 14 December 2022

Publisher's Note: MDPI stays neutral with regard to jurisdictional claims in published maps and institutional affiliations.



Copyright: © 2022 by the authors. Licensee MDPI, Basel, Switzerland. This article is an open access article distributed under the terms and conditions of the Creative Commons Attribution (CC BY) license (<https://creativecommons.org/licenses/by/4.0/>).

distance of 2.2–2.3 Å with four water molecules was found. They also reanalyzed the data of [6]. Regarding the hydrolysis products, potentiometric titrations suggested the existence of the species $\text{Sn}_3(\text{OH})_4^{2+}(\text{aq})$, in addition to $\text{Sn}_2(\text{OH})_2^{2+}(\text{aq})$ and $\text{SnOH}^+(\text{aq})$ [8]. The crystal structure of the hydrolysis product $\text{Sn}_3\text{O}(\text{OH})_2\text{SO}_4$, which is potentiometrically equivalent to $\text{Sn}_3(\text{OH})_4^{2+}(\text{aq})$, has been determined and shown to contain the discrete $[\text{Sn}_3\text{O}(\text{OH})_2]^{2+}$ ion [9,10].

A QM/MM-MD study has also been carried out on the tin(II) ion in aqueous solution [11]. It was found that the Sn–O distance peaked at 2.5 Å, with a shoulder at 2.65 Å. Gaussian fitting indicated peaks at 2.45 Å and 2.75 Å. A coordination number of eight was found. The power spectrum of the Sn–O stretching suggested peaks at 85 and 208 cm^{-1} .

2. Materials and Methods

Calculations were performed using Gaussian 98 [12]. This program version was the first to allow the analytical frequency calculation of molecules in which core electrons are described by effective core potentials (ECPs), and thus, many variants of these were tried. The MP2 calculations use the frozen core approximation. A stepping-stone approach was used for geometry optimization, in which the geometries at the levels HF/CEP-4G, HF/CEP-31G*, HF/CEP-121G*, HF/LANL2MB, HF/LANL2DZ, and HF/SDD were sequentially optimized. For minimum energy structures, the MP2/CEP-31G* and MP2/CEP-121G* calculations were also performed. Calculations were also carried out using the 6-31G* and 6-31+G* basis sets on the atoms of the water molecules (5d) with an effective core potential and basis set on the metal ion (denoted as ECP+6-31G* or 6-31+G*). For shorthand, we denoted the mixed basis sets as follows: CEP-121G* on Sn and 6-31G* on O, H, as basis set A; LANL2DZ on Sn and 6-31G* on O, H, as basis set B; and SDD on Sn and 6-31G* on O, H, as basis set C. The corresponding basis sets with diffuse functions were indicated by adding a “+” to the basis set name. Default optimization specifications were normally used. After each level, where possible, a frequency calculation was performed at the same level, and the resulting Hessian was used in the following optimization. Z-matrix coordinates constrained to the appropriate symmetry were used as required to speed up the optimizations. Since frequency calculations are done at each level, any problems with the Z-matrix coordinates would manifest themselves by giving imaginary frequencies corresponding to modes orthogonal to the spanned Z-matrix space. The Hessian was evaluated at the first geometry (opt = CalcFC) for the first level in a series in order to aid geometry convergence. We note that, for the heavy elements only, the three different CEP basis sets are equivalent (CEP-121G*) but differ for the oxygen and hydrogen atoms. We also note that the choice of core electrons defining the pseudopotential depends on the specific core potential (CEP and LANL2, [Kr]4d¹⁰; SDD, [Ar]3d¹⁰). In some cases, Gaussian 03 [13] and Gaussian 16 [14] were used to correct errors and omissions.

In many cases to follow, the symmetry of the minimum-energy complexes was the same as those previously found for bismuth [15]. To confirm these results, starting with high symmetry structures, systematic desymmetrization along the various irreducible representations was carried out [16,17]. We did not employ an implicit solvation model or additional electron correlation treatments for reasons described previously in [4]. The energies of all structures are found in Table S1.

3. Results

3.1. A Survey of Structures

Tin(II), as a lighter element in the same group as lead(II), might be expected to show similar properties. The point group symmetry for mono- through hexaaquatin(II) was usually found to be C_{2v} , C_2 , C_3 , C_2 , C_s , and C_3 . The diaquatin(II) species, like lead, ascends in symmetry to a planar C_{2v} structure at HF/LANL2MB. The tetraaquatin(II) species has C_{2v} symmetry at HF/LANL2DZ and C_s symmetry at HF/LANL2MB. The pentaqua species has C_2 symmetry at HF/LANL2MB. At all levels for the pentaqua species, if the pentacoordinate [5+0] species exists, it is competitive in energy with the [4+1], and

the most stable form is dependent on the level of theory. For the hexaaquatin(II), the C_3 [3+3] form was always more stable than the C_3 [6+0] form, which occasionally had imaginary frequencies or reverted to the [3+3] form. We did not find stable hepta-, octa-, or enneaquatin(II) structures. At the HF levels, the [6+12] form always contained at least an imaginary T mode.

The results of the systematic desymmetrization procedure [16] for aquatin(II) are as follows (see Figures 1 and S1):

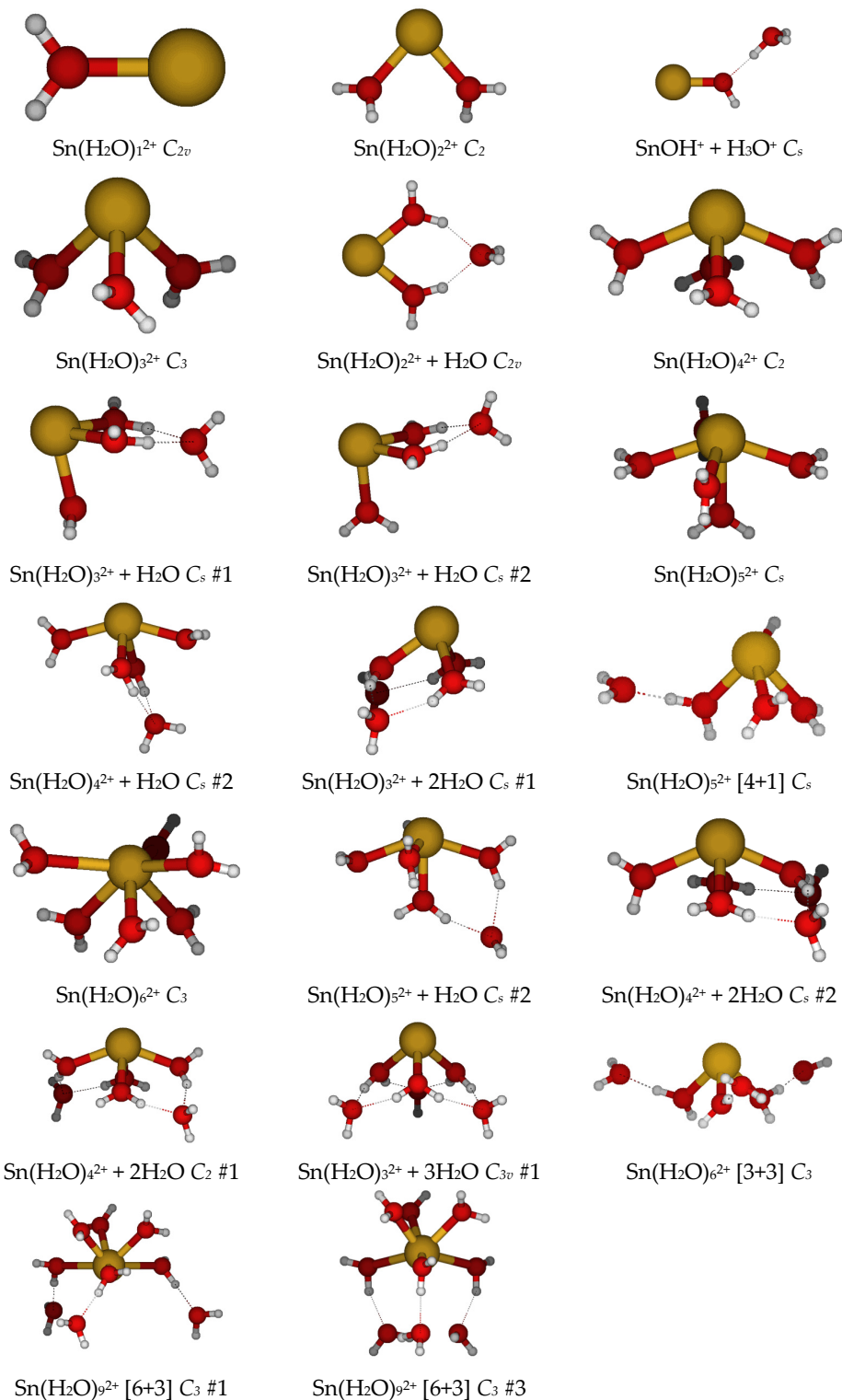


Figure 1. The minimum energy structures of aquatin(II).

- The monoaquatin(II) remained as C_{2v} at all levels;
- The most stable diaquatin(II) remained as the bent C_2 at all levels except HF/LANL2MB (C_{2v} planar). The linear holodirected D_{2d} structure was approximately 50 kJ/mol higher in energy, but the unstable bent C_s structure was only slightly higher in energy (<1 kJ/mol for nonminimal basis sets). All attempts to generate a [1+1] structure instead resulted in proton transfer to give a $\text{SnOH}^+ + \text{H}_3\text{O}^+$ complex, which was 25–40 kJ/mol higher in energy;
- The most stable triaquatin(II) remained as the pyramidal C_3 at all levels. The two pyramidal C_{3v} structures were 12–25 kJ/mol higher in energy, whereas the planar holodirected D_{3h} and D_3 structures were 60–90 kJ/mol higher in energy. The stable [2+1] C_{2v} structure was 25–50 kJ/mol higher in energy;
- The most stable tetraaquatin(II) was usually the see-saw C_2 , but it could be the C_{2v} #3 (HF/LANL2DZ, HF/B+) or C_s (HF/LANL2MB). The C_{2v} #3 was slightly higher in energy (<2 kJ/mol), with the other C_{2v} structures being higher (15–25 kJ/mol). The holodirected D_{2d} #1, #2, S_4 , and D_2 structures were much higher in energy (50–80 kJ/mol). The C_s #2 [3+1] structure was always competitive in energy, and usually lower, than the tetracoordinate structure;
- The most stable pentaquatin(II) was the square pyramidal C_s (if it exists), which is closely related to the C_{2v} #1 structure (<3 kJ/mol). The other three C_{2v} structures were ~25 kJ/mol higher in energy. The stable [4+1] and [3+2] structures were competitive in energy, and sometimes lower, depending on level of theory;
- The most stable hexaquatin(II) was the distorted octahedral C_3 (if it exists). The octahedral T_h structure was ~30 kJ/mol higher in energy;
- Of the 16 different C_{2v} heptaquatin(II) structures tried, none were stable, and either possessed imaginary modes or dissociated to a [6+1], [5+2], or [4+3] structure. Structures #1–#4, and #11, always dissociated. Structures #5–#8, and #16, usually remained as 7-coordinates. The remaining structures usually dissociated at most levels. Of the 7-coordinate C_{2v} structures, #8 and #16 were the lowest in energy. All of the 7-coordinate structures dissociated at HF/LANL2MB. Upon desymmetrization of the remaining 7-coordinate C_{2v} structures to C_2 , nearly all dissociated to [6+1], [5+2], or [4+3] structures. The only exceptions, C_2 #10 and #15 at HF/CEP-31G*, possessed imaginary B modes, of which one corresponds to a water molecule moving to the second hydration shell;
- Of the octaquatin(II) structures, two D_{4h} and two D_{4d} structures (point group order $h = 16$) were first examined. Multiple imaginary modes were present;
 - For the D_{4d} #1 and #2 structures, desymmetrization along the A_2 imaginary mode gave the same S_8 structure; along the B_1 imaginary mode, they gave the same D_4 #2 structure; along the B_2 imaginary mode, they gave the C_{4v} #1 and #2 structures; and along the imaginary E_1 mode, they gave the same C_{2v} #1 structure (via C_s);
 - For the D_{4h} #1 and #2 structures, desymmetrization along the A_{1u} imaginary mode gave the D_4 #2 structure found before; along the A_{2g} imaginary mode, they gave the same C_{4h} #1 structure; along the A_{2u} imaginary mode, they gave the C_{4v} #3 [4+4] and #4 structures; along the B_{2g} imaginary mode (D_{4h} #1), the D_{2h} #1 structure ascended in symmetry to D_{4h} #2; along the B_{1g} (D_{4h} #2) imaginary mode, they gave the D_{2h} #2 structure; along the B_{1u} imaginary mode, they gave the same D_{2d} #1 structure; along the B_{2u} mode, they gave the D_{2d} #2 and #4 structures, respectively; and along the E_g and E_u modes, they gave D_{2h} #3 and #4 (via C_{2h} and C_{2v});

Examination of lower symmetry structures ($h = 8$) gave the following results:

- For the S_8 #1 structure, all E_1 and B imaginary modes corresponded to the expulsion of water molecules to the second hydration shell. Desymmetrization along the B mode gave the [4+4] C_4 ;

- For the D_4 #2 structure, the E mode corresponded to the expulsion of water molecules to the second hydration shell. Desymmetrization along the A_2 mode gave either a [4+4] C_4 structure or a C_4 #2 structure, whereas along the B_1 mode, it gave the D_2 #1 structure;
- For the C_{4h} #1 structure, the imaginary E_u mode corresponded to the expulsion of two water molecules. Desymmetrization along the imaginary A_u mode for the most part gave either a [4+4] C_4 structure or ascended in symmetry to S_8 ; along the imaginary B_u mode at HF/CEP-4G and HF/LANL2MB, it gave a D_{2d} #5 and S_4 structure, respectively. This D_{2d} #5 structure was then rerun at all levels;
- For the D_{2d} structures, desymmetrization along an A_2 imaginary mode would give an S_4 structure; along a B_1 imaginary mode, they gave a D_2 structure; along a B_2 imaginary mode, they gave a C_{2v} structure; along an E mode, they gave either a C_2 or C_s structure. Along the A_2 mode, an S_4 #2 or #4 structure typically resulted, or ascension in symmetry to the D_{2d} #5; along the B_1 mode, there was usually ascension to D_4 #2; along the B_2 mode, there was dissociation to a [6+2] or [4+4] structure; and along an E mode, dissociation would occur;
- For the D_{2h} structures, desymmetrization along the imaginary A_u mode would give a D_2 structure, and along the imaginary B_{ng} modes, a C_{2h} structure was given. In all cases, these desymmetrized, and most ascended in symmetry to structures already found (D_2 #5, D_4 #2, C_{4h} #1). The B_{nu} modes corresponded to the expulsion of water molecules from the first hydration sphere;

Examination of lower symmetry structures ($h = 4$) gave the following results:

- For the C_{2v} structures, desymmetrization along the A_2 mode would give a C_2 structure, and along the B_1 or B_2 mode, different C_s structures were given. For the C_{2v} structures, at least one of the imaginary B modes in each structure corresponded to dissociation to a [6+2] structure, whereas desymmetrization along the A_2 mode led to a [4+4] or [4+2+2] structure;
- For the C_4 and S_4 structures, the imaginary E mode corresponded to dissociation to a [6+2] structure, whereas desymmetrization along the B mode to give a C_2 structure resulted in dissociation;
- For the D_2 structures, at least one of the imaginary B_2 or B_3 modes corresponded to dissociation to a [6+2] structure, whereas desymmetrization along the B_1 mode to give a C_2 structure resulted in dissociation to a [6+2] or [4+4];

Based on these results, we must conclude that a stable 8-coordinate octaaquatin(II) ion cannot exist.

- Of the enneaquatin(II) structures, four D_{3h} structures (point group order $h = 12$) were first examined. Multiple imaginary modes were present. Desymmetrization along the A_1'' mode would yield D_3 structures; along A_2' , C_{3h} structures were given; and along A_2'' , C_{3v} structures were given. A common D_3 #1 structure was found for most, and in some cases gave an additional [6+3] structure. Two possible C_{3h} structures were found, and in some cases gave an additional [6+3] structure. Four possible C_{3v} structures were found, and in some cases gave additional [6+3] structures. At least one of the degenerate modes corresponded to the expulsion of water molecule(s) from the inner coordination shell;
 - For the D_3 structure, desymmetrization along the A_2 mode gave a C_3 #1 [6+3] structure. At least one of the E modes corresponded to the loss of water molecules from the first hydration shell.
 - For the C_{3h} structures, desymmetrization along the A'' mode gave either the C_3 #1 [6+3] structure above or a new C_3 #3 [6+3] structure (or occasionally [3+3+3]). At least one of the E modes corresponded to the loss of water molecules from the first hydration shell.
 - For the C_{3v} structures, desymmetrization along the A_2 mode gave one of the C_3 [6+3] structures (or occasionally [3+3+3]) found above. At least one of the

E modes corresponded to the loss of water molecules from the first hydration shell.

Based on these results, we must conclude that a stable 9-coordinate enneaquatin(II) ion cannot exist.

To summarize these results, by using the systematic desymmetrization procedure, we have found stable structures for the mono- through hexaaquatin(II) complexes, and we have shown that hepta-, octa-, and enneaqua structures do not exist on the potential energy surface. The hexaaquatin(II) C_3 structure is only stable at HF/CEP-31G*, HF/CEP-121G*, and MP2/CEP-31G*. The pentaquatin(II) C_5 structure is not stable at HF/CEP-4G, HF/LANL2DZ, and HF/SDD. In most cases, for systems with more than three water molecules, the most stable structure on the potential energy surface is tricoordinate, with the remaining water molecules in the second hydration sphere (the main exceptions being HF/CEP-31G* and HF/CEP-121G*). These results suggest that tin(II) would be tricoordinate trigonal pyramidal in an aqueous solution.

3.2. The Sn–O Distance

The average Sn–O distance as a function of coordination number is plotted in Figure 2 for all of the levels studied. The Sn–O distance always lengthened following an increase in the coordination number. We can see some gaps for $n = 4–6$ at some levels where no local minimum existed. The Sn–O distance using the minimal basis HF/LANL2MB was shorter than the other levels at the same hydration number by 0.1–0.3 Å, which tended to cluster together. The results using CEP-31G* were nearly coincidental with those of CEP-121G*. For all levels, there was a pronounced change in slope at $n = 3$. Within the cluster noted above, the Sn–O distance using the SDD basis set/pseudopotential on Sn (HF/SDD, HF/C, HF/C+) tended to be the longest ($n = 1–5$, 2.20–2.50 Å), whereas those using the LANL2DZ basis set/pseudopotential on Sn (HF/LANL2DZ, HF/B, HF/B+) were the shortest. This differed for lead, where the CEP basis set/pseudopotential tended to be the shortest [4]. The effect of the basis set/pseudopotential combination was more important than the presence or absence of correlation (HF vs. MP2). Metal–oxygen bond lengths to those oxygens making a smaller angle to the principal symmetry axis were longer, as was noted previously for aqualead(II) [4].

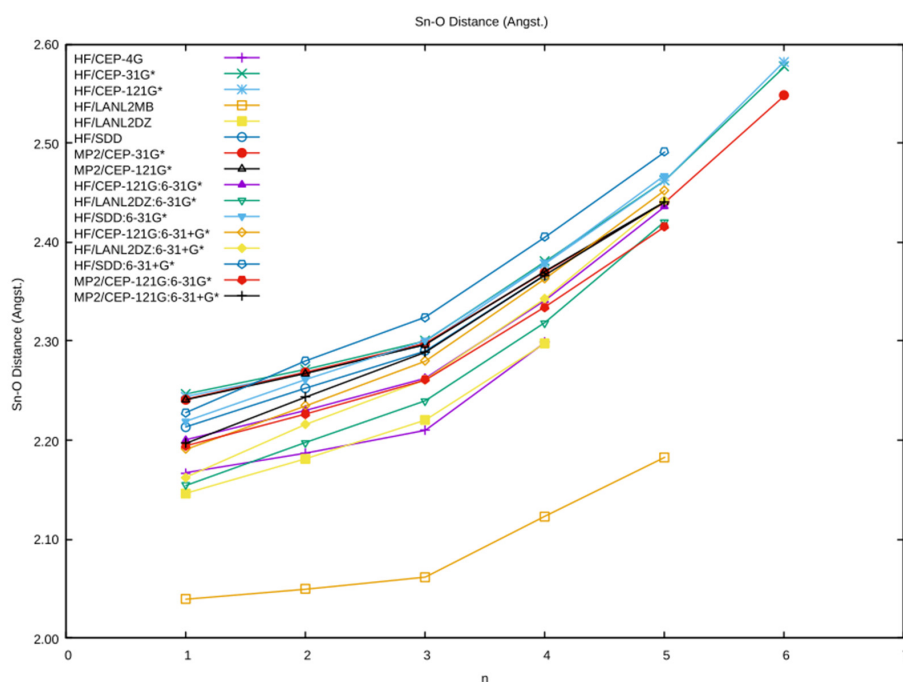


Figure 2. The dependence of the average Sn–O distance on the coordination number n and level of theory.

3.3. The Sn–O Vibrational Frequency

The vibrational frequency of the totally symmetric Sn–O stretch as a function of coordination number is plotted in Figure 3. As expected, the frequencies at the minimal basis HF/LANL2MB were much higher than the other levels which clustered together. For the most part, the vibrational frequency decreased as a function of hydration number. There was a levelling effect upon going from $n = 4$ to $n = 5$, because, for the square pyramidal $n = 5$, the character of the mode changed to be predominantly a Sn–O_{apex} stretch. The results using CEP-31G* were nearly coincidental with those of the CEP-121G*, and the MP2 values were $\sim 15 \text{ cm}^{-1}$ higher than the HF values. The addition of diffuse functions (A+ vs. A) lowered the vibrational frequency by $\sim 30 \text{ cm}^{-1}$, and correlation increased it by $\sim 5\text{--}15 \text{ cm}^{-1}$. This was also true for the mixed basis set calculations. All other things being equal, the LANL2DZ frequencies were the highest, and the CEP frequencies were the lowest, with the SDD frequencies falling in the middle. The inverse relationship between average bond length and symmetric stretching frequency can be clearly seen.

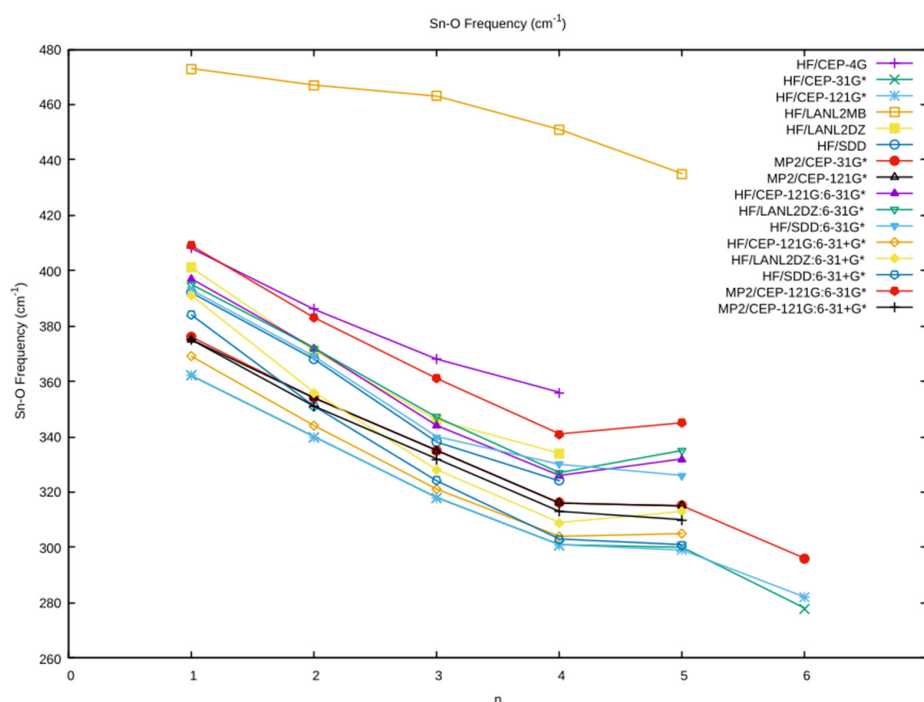


Figure 3. The dependence of the totally symmetric Sn–O frequency on the coordination number n and level of theory.

4. Discussion

Because of the lack of experimental data on aquatin(II) complexes, certainty regarding the structure and vibrational frequencies of the aquatin(II) is lacking. We may compare a series of structures, such as $[n+0]$ and $[(n-m)+m]$. For a hydration number of three, the tricoordinate $[3+0]$ is always more stable than the $[2+1]$ structure. For a hydration number of four, the tricoordinate $[3+1]$ is usually more stable than $[4+0]$, except for HF/CEP-31G* and HF/CEP-121G*, but they are competitive in energy. For a hydration number of five, the $[4+1]$ and $[3+2]$ structures are usually more stable than the $[5+0]$, except for HF/CEP-31G* and HF/CEP-121G*, but all are still competitive in energy. For a hydration number of six, the $[4+2]$ structure seems to be the most stable, with the $[3+3]$ structure being competitive in energy. The picture emerging is that of a variable coordination number between three and six, with three (trigonal pyramidal) and four (see-saw) being the most likely.

We recently became aware [18] of a crystal structure determination of an aquatin(II) ion in the compound tin(II) perchlorate trihydrate [19]. The Sn–O distance was reported to be $2.201(7) \text{ \AA}$. Examination of Figure 2, at $n = 3$, and Table 1 suggest that, if crystal packing forces are negligible, then the MP2/A+, HF/LANL2DZ, and HF/B+ levels give excellent

agreement with the experiment. This result was confirmed by Persson and co-workers, who obtained 2.208(9) Å and obtained EXAFS results for the crystal and solution Sn–O distance of 2.209(3) and 2.219(3) Å, respectively, which quite importantly shows that the solution structure of tin(II) is the same as the solid. The LAXS measurement gives, at 2.206(2) Å, nearly the same value for the Sn–O distance [20].

Table 1. Bond lengths (Å) of triaquatin(II). The theoretical levels A, B, and C are described in the text. HF = Hartree-Fock, MP2 = second-order Møller-Plesset, Expt. = experiment, XRD = X-ray diffraction, EXAFS = Extended X-ray absorption fine structure, LAXS = Large angle X-ray scattering.

Basis Set/Pseudopotential	HF	MP2
CEP-4G	2.2098	n/c
CEP-31G*	2.3001	2.2978
CEP-121G*	2.2963	2.2964
LANL2MB	2.0616	n/c
LANL2DZ	2.2202	n/c
SDD	2.2898	n/c
A	2.2624	2.2606
B	2.2397	n/c
C	2.3005	n/c
A+	2.2797	2.2887
B+	2.2610	n/c
C+	2.3241	n/c
Expt. XRD [19]		2.201(7)
Expt. XRD [20]		2.208(9)
Expt. EXAFS xtal. [20]		2.209(3)
Expt. EXAFS soln. [20]		2.219(3)
Expt. LAXS soln. [20]		2.206(2)

The vibrational frequency for the $n = 3$ structure lay in the range 320–370 cm^{-1} . The effect of a second hydration sphere should be to increase this value somewhat. For most octahedral metal ions that we have previously examined, a rough rule of thumb is that, upon including a second hydration sphere, the vibrational frequency increases by $20q \text{ cm}^{-1}$, where q is the total charge on the octahedral ion. For tin(II), comparison of the vibrational frequencies of $[\text{Sn}(\text{H}_2\text{O})_3]^{2+} C_3$, and $[\text{Sn}(\text{H}_2\text{O})_3]^{2+} \cdot (\text{H}_2\text{O})_3 C_{3v}$ revealed a large $\sim 85 \text{ cm}^{-1}$ increase in the vibrational frequency. This suggests that tin(II) should have an observable band in the isotropic Raman spectra corresponding to the totally symmetric stretching motion in the range of 400–450 cm^{-1} .

5. Conclusions

The common CEP, LANL2DZ and SDD pseudopotentials were paired with various basis sets to study the hydrated tin(II) ion. The calculations using minimal basis sets performed poorly. For the most part, the calculated structures were consistent with recent experimental results of a tricoordinate trigonal pyramidal hemidirected aqua complex. The careful use of symmetry can be used to both guide the search for new structures and also to rule out structures.

Supplementary Materials: The following are available online at <https://www.mdpi.com/article/10.3390/liquids2040027/s1>, Figure S1: Some stationary point (non-minimum) energy structures of aquatin(II); Table S1: Total Energies of Aquatin(II) Species.

Author Contributions: Conceptualization, C.C.P.; methodology, C.C.P.; investigation, C.M.G. and C.C.P.; resources, C.C.P.; data curation, C.C.P.; writing—original draft preparation, C.C.P.; writing—review and editing, C.C.P.; visualization, C.C.P.; supervision, C.C.P.; project administration, C.C.P.; funding acquisition, C.C.P. All authors have read and agreed to the published version of the manuscript.

Funding: This research was funded by the Natural Sciences and Engineering Research Council of Canada.

Data Availability Statement: Data is contained within the article and Supplementary Materials.

Acknowledgments: The authors thank the Department of Astronomy and Physics, at Saint Mary's University (AP-SMU), for providing access to computing facilities, in particular to cygnus, a 10-processor Sun server, which was purchased with assistance from the Canada Foundation for Innovation, Sun Microsystems, the Atlantic Canada Opportunities Agency, and SMU. CCP also thanks ACEnet and Compute Canada for providing access to computers and Gaussian 03/16. CCP acknowledges the former financial support of the NSERC. CMG acknowledges the support of the Department of Economic Development (Government of Nova Scotia), the Office of the Dean of Science, SMU, and the Cooperative Education program (SMU–Work Term 2, Fall 2001 and Work Term 3, Winter 2002).

Conflicts of Interest: The authors declare no conflict of interest. The funders had no role in the design of the study; in the collection, analyses, or interpretation of data; in the writing of the manuscript, or in the decision to publish the results.

References

1. Richens, D.T. *The Chemistry of Aqua Ions*; Wiley: Chichester, UK, 1997.
2. Baes, C.F., Jr.; Mesmer, R.E. *The Hydrolysis of Cations*; Wiley: New York, NY, USA, 1976.
3. Pye, C.C.; Gunasekara, C.M. An Ab Initio Investigation of the Hydration of Thallium(III) and Mercury(II). *J. Solution Chem.* **2020**, *49*, 1419–1429. [[CrossRef](#)]
4. Pye, C.C.; Gunasekara, C.M. An Ab Initio Investigation of the Hydration of Lead(II). *Liquids* **2022**, *2*, 39–49. [[CrossRef](#)]
5. Cox, H.; Stace, A.J. Molecular View of the Anomalous Acidities of Sn^{2+} , Pb^{2+} , and Hg^{2+} . *J. Am. Chem. Soc.* **2004**, *126*, 3939–3947. [[CrossRef](#)]
6. Johansson, G.; Ohtaki, H. An X-Ray Investigation of the Hydrolysis Products of Tin(II) in Solution. *Acta Chem. Scand.* **1973**, *27*, 643–660. [[CrossRef](#)]
7. Yamaguchi, T.; Lindqvist, O.; Claeson, T.; Boyce, J.B. EXAFS and X-ray diffraction studies of the hydration structure of stereochemically active Sn(II) ions in aqueous solution. *Chem. Phys. Lett.* **1982**, *93*, 528–532. [[CrossRef](#)]
8. Tobias, R.S. Studies on the Hydrolysis of Metal Ions. 21. The Hydrolysis of the Tin(II) Ion, Sn^{2+} . *Acta Chem. Scand.* **1958**, *12*, 198–223. [[CrossRef](#)]
9. Grimvall, S. On the Crystal Structure of $\text{Sn}_3\text{O}(\text{OH})_2\text{SO}_4$. *Acta Chem. Scand.* **1973**, *27*, 1447. [[CrossRef](#)]
10. Davies, C.G.; Donaldson, J.D.; Laughlin, D.R.; Howie, R.A.; Beddoes, R. Crystal structure of tritin(II) dihydroxide oxide sulfate. *J. Chem. Soc. Dalton Trans.* **1975**, 2241–2244. [[CrossRef](#)]
11. Hofer, T.S.; Pribil, A.B.; Randolph, B.R.; Rode, B.M. Structure and Dynamics of Solvated Sn(II) in Aqueous Solution: An ab Initio QM/MM MD Approach. *J. Am. Chem. Soc.* **2005**, *127*, 14231–14238. [[CrossRef](#)] [[PubMed](#)]
12. Frisch, M.J.; Trucks, G.W.; Schlegel, H.B.; Scuseria, G.E.; Robb, M.A.; Cheeseman, J.R.; Zakrzewski, V.G.; Montgomery, J.A., Jr.; Stratmann, R.E.; Burant, J.C.; et al. *Gaussian 98, Revision A.9*; Gaussian, Inc.: Pittsburgh, PA, USA, 1998.
13. Frisch, M.J.; Trucks, G.W.; Schlegel, H.B.; Scuseria, G.E.; Robb, M.A.; Cheeseman, J.R.; Montgomery, J.A., Jr.; Vreven, T.; Kudin, K.N.; Burant, J.C.; et al. *Gaussian 03, Revision D.02*; Gaussian, Inc.: Wallingford, CT, USA, 2004.
14. Frisch, M.J.; Trucks, G.W.; Schlegel, H.B.; Scuseria, G.E.; Robb, M.A.; Cheeseman, J.R.; Scalmani, G.; Barone, V.; Petersson, G.A.; Nakatsuji, H.; et al. *Gaussian 16, Revision A.03*; Gaussian, Inc.: Wallingford, CT, USA, 2016.
15. Pye, C.C.; Gunasekara, C.M.; Rudolph, W.W. An ab initio investigation of bismuth hydration. *Can. J. Chem.* **2007**, *85*, 945–950. [[CrossRef](#)]
16. Pye, C.C.; Whynot, D.C.M.; Corbeil, C.R.; Mercer, D.J. Desymmetrization in geometry optimization: Application to an ab initio study of copper(I) hydration. *Pure Appl. Chem.* **2020**, *92*, 1643–1654. [[CrossRef](#)]
17. Pye, C.C.; Gilbert, C.R. An ab initio investigation of the second hydration shell of metal cations. *Comput. Appl. Chem.* **2020**, *208*, 395–397. [[CrossRef](#)]
18. Persson, I. Structures of Hydrated Metal Ions in Solid State and Aqueous Solution. *Liquids* **2022**, *2*, 210–242. [[CrossRef](#)]
19. Hennings, E.; Schmidt, H.; Kohler, M.; Voigt, W. Crystal structure of tin(II) perchlorate trihydrate. *Acta Crystallogr. E* **2014**, *70*, 474–476. [[CrossRef](#)] [[PubMed](#)]
20. Persson, I.; D'Angelo, P.; Lundberg, D. Hydrated and Solvated Tin(II) Ions in Solution and the Solid State, and a Coordination Chemistry Overview of the $d^{10}s^2$ Metal Ions. *Chem. Eur. J.* **2017**, *22*, 18583–18592. [[CrossRef](#)] [[PubMed](#)]